Journal of Fluorescence (2022) 32:1289–1297
https://doi.org/10.1007/s10895-022-02973-8

RESEARCH

Modification-Free Fluorescent Biosensor for CEA Based on Polydopamine-Coated Upconversion Nanoparticles

Dezhong Yu[1,2] · Zhonghui Zha[1,2] · Sheng Tang[1,2] · Yuan Qiu[1,2] · Dong Liu[1,2]

Received: 24 March 2022 / Accepted: 13 May 2022 / Published online: 21 May 2022

Abstract

Upconversion nanoparticles (UCNPs) have achieved considerable success in protein sensing in vitro. And aptamer is one of the most frequently used biomolecules to modify the nanoparticles for protein assay. However, the complicated process of modifying UCNPs with DNA and the susceptibility of the phosphate groups of DNA backbone to adsorb on the surface of UCNPs have limited their practical applications. To overcome these limitations, a modification-free fluorescent biosensor based on polydopamine-coated upconversion nanoparticles (UCNPs@PDA) is proposed. It consists of UCNPs@PDA and CEA aptamer-functionalized AuNPs (AuNPs-CEA aptamer). The CEA aptamer on AuNPs can be adsorbed onto the surface of UCNPs@PDA due to the interactions of π–π stacking and hydrogen bonding, triggering the process of fluorescence resonance energy transfer (FRET) from UCNPs@PDA to AuNPs-CEA aptamer. In the presence of CEA, the AuNPs-CEA aptamer departs from UCNPs@PDA due to the stronger affinity of CEA with its aptamer. Therefore, the recovery of upconversion fluorescence can sensitively quantify the concentration of CEA. This biosensor provides a linear range from 0.1 to 100 ng/mL for CEA with a LOD of 0.031 ng/mL in an aqueous solution. In spiked human serum samples, the same linear range is acquired with a slightly higher LOD of 0.055 ng/mL, demonstrating the great potential of the biosensor in practical application.

Keywords Fluorescence · Biosensor · Upconversion nanoparticles · Aptamer · Polydopamine

Introduction

Lanthanide-doped upconversion nanoparticles (UCNPs), which generate anti-Stokes emission under near-infrared excitation, can avoid the auto-fluorescence of background and scattered light of biological samples [1–3]. These properties make UCNPs promising energy donors in the process of fluorescence resonance energy transfer (FRET) [2]. A series of biosensors have been developed based on this principle to detect metal ions [4], nucleic acids [5],proteins and so on [6].

Aptamer, a short single-stranded nucleotide obtained by in vitro selection [7, 8], can act as recognition elements in biosensing [9–11]. Aptamer can be easily tagged with fluorescent dyes, drugs, and nanoparticles in biosensors [12–14]. Up to now, a variety of UCNPs-based protein biosensors have been constructed with the use of aptamers [15, 16]. However, utilizing UCNPs in biosensing often requires complex hydrophilic treatment because UCNPs are normally synthesized in organic solvents and functionalized with hydrophobic ligands [17]. Therefore, the results of detection are inevitably influenced by the efficiency of conjugation between UCNPs and aptamers. Although various coupling methods have been proposed, there still exists a ceiling of coupling efficiency which is currently being reported as less than 10% [18]. Another major barrier is that the strong affinity between lanthanide ions on the surface of UCNPs and phosphate groups of DNA backbone [19], which impairs the ability of the aptamer to recognize the target.

To overcome these problems, we herein developed a modification-free strategy by coating UCNPs with a polydopamine (PDA) shell. PDA is a reported polymer that can

✉ Dong Liu
liudong1980@aliyun.com

[1] School of Chemistry and Environmental Engineering, Wuhan Institute of Technology, Wuhan 430205, People's Republic of China

[2] Engineering Research Center of Phosphorus Development and Utilization of Ministry of Education, Wuhan Institute of Technology, Wuhan 430205, People's Republic of China

independently modify the surface of various nanomaterials [20]. One particular excellent feature of PDA molecule is that it has abundant amino groups and catechol, which makes it possible to be further functionalized with various biomolecules on its surface [21]. More importantly, PDA with a large number of aromatic groups can be assembled with π electron-rich biomolecules, such as DNA, through the interactions of π-π stacking and hydrogen bonding [22]. In order to improve the efficiency of coupling between UCNPs and aptamer, and to prevent the phosphate groups of DNA backbone from binding directly with lanthanide ions on the surface of UCNPs, we utilized the PDA-coated UCNPs (UCNPs@PDA) to fabricate the biosensor to analyze carcinoembryonic antigen (CEA), which is a critical protein playing great roles in many kinds of cancer, especially colorectal cancer [23].

Herein, UCNPs@PDA without modification is used as the energy donor, and CEA aptamer-labled gold nanoparticles (AuNPs-CEA aptamer) served as energy acceptor. AuNPs, with a high molar extinction coefficient and easy assembly with DNA, are usually used as efficient energy acceptors in FRET biosensors [24, 25]. The AuNPs-CEA aptamer complex were readily adsorbed onto the surface of the UCNPs@PDA via the interactions of π–π stacking and hydrogen bonding, leading to quenching of the upconversion fluorescence. In the presence of CEA, the distance from UCNPs@PDA to AuNPs-CEA aptamer was increased due to the stronger affinity between aptamer and CEA, which blocked the FRET process and thus the fluorescence of UCNPs recovered in a CEA concentration-dependent manner.

Material and Methods

Materials

1-Octadecene and dopamine hydrochloride were acquired from Aladdin Reagent, Ltd. (Shanghai, China). CEA was obtained from Linc-Bio Science Co., Ltd (Shanghai, China). The sulfydryl modified CEA aptamer (5'-SH-AAAAAATACCAGCTTATTCAATT-3') was purchased from Sangon Biotechnology Co., Ltd. (Shanghai, China). Fresh human serum samples were obtained from hospital. Other chemical reagents were purchased from Sinopharm Chemical Reagent Co., Ltd. (Shanghai, China). All chemicals were of analytical grade or higher grade and used without further purification. All aqueous solutions used in this experiment were prepared by ultrapure water (Mill -Q, Millipore, 18.2 MΩ resistivity).

Instrumentations

Transmission electron microscopy (TEM) images of UCNPs, UCNPs@PDA and AuNPs were taken on Hitachi H-7000FA at 75 kV. X-Ray Diffractometer (XRD) spectrum was recorded with XPert Pro. UV–vis spectra were recorded with a UV-2550 spectrophotometer (Shimadzu, Japan). The upconversion luminescence spectra were acquired by a RF-5301 fluorophotometer (Shimadzu, Japan) using an external 980 nm CW laser as excitation source (Beijing Hi-Tech Optoelectronic Co., Ltd.).

Synthesis of UCNPs@PDA

Synthesis of UCNPs The $NaYF_4$:Yb,Tm nanoparticles were synthesized according to a co-precipitation method [26]. 4.4 mL of oleic acid, 12.4 mL of 1-octadecene and 0.8 mmol of $Ln(oleate)_3$ were add into a three-necked flask with constant stirring. After heating to 50° C, 10 mL of methanol solution containing 2 mmol of NaOH and 3.2 mmol of NH_4F was added and allowed for reaction for 30 min. Under the protection of argon atmosphere, the temperature was then raised to 100° C. Until the residual methanol solution in the flask was evacuated, the temperature was raised to 290° C and kept for 90 min. Naturally cooling down to room temperature, and centrifuging by adding ethanol to obtain a precipitate. A mixed solution of cyclohexane / ethanol at a ratio of 1: 2 (v/v) was used to wash the precipitate for twice and the product OA-UCNPs were dispersed in cyclohexane and stored under 4° C.

Coat UCNPs with PDA The coating was conducted referring to the literature [27]. 0.65 mL of Igepal CO-520 was added to 10 mL of cyclohexane which contained 10 mg of OA-UCNPs. 75 μL of 28 wt% ammonium hydroxide was added into the mixture after stirring for 20 min, followed by sonication for 15 min. After another stirring for 30 min, under a rate of 3 μL / min, 50 μL of 25 wt% dopamine hydrochloride aqueous solution was injected into the mixture and stirred for 1 h. Then ethanol was added to precipitate the nanoparticles. Finally, after washing with ethanol and water for three times by centrifugation (12,000 rpm, 15 min), the UCNPs@PDA was dispersed in water.

Synthesis of AuNPs-CEA Aptamer

Synthesis of AuNPs The synthesis of AuNPs with the size of about 13 nm was according to the literature [28]. 50 mL of 1 mM $HAuCl_4$ aqueous solution was added into a two-necked

flask and heated to 140° C under stirring and reflux. 5 mL of 38.8 mM trisodium citrate solution was quickly injected into the boiling solution and the mixture was kept for reaction for 15 min under reflux. The mixture was filtered through a 0.22 μm sterile syringe filter after naturally cooling down to room temperature. According to the literature [28], the concentration of the synthesized AuNPs was calculated to be 3 nM by the UV–visible absorption spectra of AuNPs.

Modify AuNPs with CEA aptamer According to the literature [29], all the following experiments were carried out in the dark. Firstly, the disulfide bond of 1 nmol of CEA aptamer was cleaved by adding 5 nmol tris (2-carboxyethyl) phosphine (TCEP) and incubating for 1 h at room temperature. After freshly cleaved CEA aptamer was added into 3.3 mL of AuNPs, the mixture was stirred for 16 h at room temperature. Adding 10 μL of 2 M NaCl solution at a rate of 5 min / time into the mixture until the final NaCl concentration reached 60 mM. After stirring for 24 h, the product was collected by centrifugation and washed with water for three times. At last, the AuNPs-CEA aptamer was resuspended in 0.1 mL of Tris–HCl (10 mM, 50 mM NaCl, pH 7.4) buffer and its concentration was considered to be 100 nM.

Optimization of the Biosensor

Confirm the stability of UCNPs@PDA 0.04 mg/mL of UCNPs@PDA was incubated in Tris–HCl buffer (10 mM, pH 7.4) at 37° C for different times (0, 5, 10, 20, 40, 60, 80, 100, 120 min), then these mixtures were subject to upconversion fluorescence measurements.

Confirm the concentration of AuNPs-CEA aptamer A fixed amount of UCNPs@PDA of 0.04 mg/mL was respectively incubated with different concentration of AuNPs-CEA aptamer (0, 1.39, 2.77, 4.85, 6.93, 10.4 nM) in Tris–HCl buffer (10 mM, pH 7.4) at 37° C for 90 min, then these mixtures were subject to upconversion fluorescence measurements.

Confirm the time of fluorescence quenching 0.04 mg/mL of UCNPs@PDA and 10.4 nM of AuNPs-CEA aptamer were incubated in Tris–HCl buffer (10 mM, pH 7.4) at 37° C for different times (0, 5, 20, 40, 60, 90 min), then the intensity of upconversion fluorescence was measured.

CEA Detection in Aqueous Solution

0.04 mg/mL of UCNPs@PDA and various concentrations of CEA (0, 0.1, 0.5, 1, 5, 8, 10, 30, 70, 100 ng / mL) were mixed in Tris–HCl buffer (10 mM, pH 7.4) and incubated at 37° C for 90 min. Then 10.4 nM of AuNPs-CEA aptamer was respectively added to these mixtures and incubated at 37° C for 90 min. Finally, the intensity of upconversion fluorescence was measured.

Specificity Assessment of the Biosensor

0.04 mg/mL of UCNPs@PDA and 100 ng / mL of Ca^{2+}, Na^{+}, L-Cys, glucose, BSA, albumin, AFP and CEA were respectively mixed in Tris–HCl buffer (10 mM, pH 7.4) and incubated at 37° C for 90 min. Then 10.4 nM of AuNPs-CEA aptamer was added to these mixtures to further incubate at 37° C for 90 min. Finally, the intensity of upconversion fluorescence was measured.

CEA Detection in Human Serum

The human serum samples were firstly 100-fold diluted with Tris–HCl buffer (10 mM, pH 7.4). 0.04 mg/mL of UCNPs@PDA and various concentrations of CEA (0, 0.1, 0.5, 1, 5, 8, 10, 30, 70, 100 ng / mL) were respectively added into the diluted serum and incubated at 37° C for 90 min. Then 10.4 nM of AuNPs-CEA aptamer was added to these mixtures and incubated at 37° C for 90 min. Finally, the intensities of upconversion fluorescence were measured.

The five tumour patients' serum samples were also firstly 100-fold diluted with Tris–HCl buffer (10 mM, pH 7.4), and the concentration of CEA became 0.83, 1.31, 2.79, 4.70 and 6.98 ng/mL. 0.04 mg/mL of UCNPs@PDA and 50 ng / mL of CEA were respectively added into the diluted serum and incubated at 37° C for 90 min. Then 10.4 nM of AuNPs-CEA aptamer was added to these mixtures and incubated at 37° C for 90 min, followed by measurements of the intensity of upconversion fluorescence.

Results and Discussion

Principles of the Biosensor for CEA Detection

As shown in Fig. 1, the synthesized AuNPs have a wide absorption band in the wavelength from 700 to 300 nm, and the peak of absorption is located at 520 nm. The emission of $NaYF_4$:Yb,Tm nanoparticles is located at 480 nm, which can overlap well with the absorption of AuNPs and meet the requirements of FRET. According to a large number of studies [29], AuNPs not only possess high extinction coefficient, but also are easy to be modified with aptamer, exactly meeting the requirements for energy acceptor. Therefore, we chose the CEA aptamer modified AuNPs as the energy acceptor of UCNPs@PDA to construct the biosensor for CEA analysis.

The principle of the as-developed sensor is shown in Scheme1. Taking the advantage of the interactions of π–π stacking and hydrogen bonding between PDA and aptamer, CEA aptamer on the surface of AuNPs can be adsorbed onto UCNPs @ PDA,

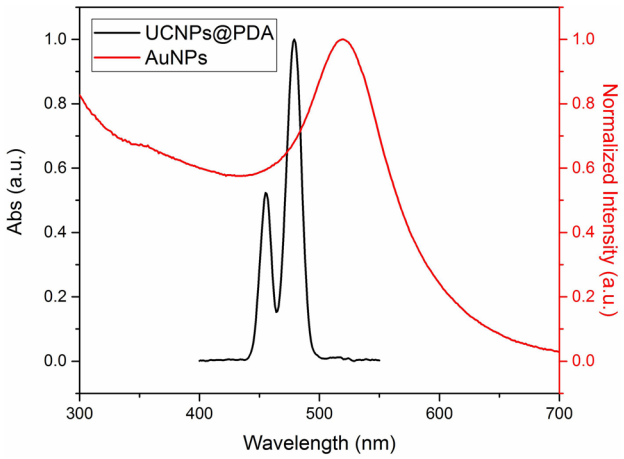

Fig. 1 Emission spectra of UCNPs @ PDA (black line) and UV–vis absorption of AuNPs (red line)

leading to the quenching of the upconversion fluorescence, which not only improves the efficiency of coupling between UCNPs and aptamers, but also prevents the phosphate groups on backbone of DNA from binding directly with lanthanide ions on the surface of UCNPs. In the presence of CEA, the AuNPs-CEA aptamer would be separated from UCNPs @ PDA because the aptamer has stronger affinity with CEA than PDA. The breaking of energy donor/acceptor assembly causes the recovery of upconversion fluorescence, thus the concentration of CEA can be determined.

Characterization of UCNPs and UCNPs@PDA

The UCNPs were analyzed using X-ray diffraction (XRD) characterization, which confirmed the UCNPs were hexagonal phases, and the intensity and position of the diffraction peaks were consistent with standard pure hexagonal $NaYF_4$ crystals (Fig. 2a). The transmission electron microscopy (TEM) image, as shown in Fig. 2b, indicated the prepared OA-UCNPs were spheres with a uniform size of about 26 nm. According to the literature, the coating of UCNPs with PDA applied a water-in-oil microemulsion method [27].Due to the strong adhesion of PDA to the surface of nanomaterials, it was easy to coat UCNPs with PDA. The coating of PDA enables UCNPs to convert from oil-soluble to water-soluble, which is favorable for subsequent biosensing applications. From the result of the X-ray electron spectroscopy (XPS) test (Fig. 2c), there was a clear peak of N at UCNPs@PDA, proving the coating of PDA was successful. TEM analysis further revealed the successful coating of PDA, which showed that a shell was attached to the surface of the UCNPs with the thickness of about 3 nm (Fig. 2d).

Characterization of AuNPs and AuNPs-CEA Aptamer

It can be seen from the TEM image that the obtained citrate modified AuNPs had a relatively uniform size of about 13 nm with good water dispersibility (Fig. 3a). After the conjugation with CEA aptamer, the absorption peak of AuNPs-CEA aptamer has a slight red-shift for about 3 nm and showed a significant DNA absorption peak at 260 nm in the UV–vis absorption spectrum (Fig. 3b). Moreover, the AuNPs-CEA aptamer possessed very good solubility and could even remain stable in aqueous solution for a month, which is beneficial for bioassays. More evidence of the successful coupling between AuNPs and CEA aptamer was found in the measurement of zeta-potential, as shown in Fig. S1.† The AuNPs-CEA aptamer conjugate was determined to be -17.2 mV, obviously negative-shifted as compared with that of the citrate modified AuNPs (-8.30 mV).

Optimization of experimental conditions

Before the assay of CEA, a series of conditions in experiment were optimized to make sure the biosensor performed in the best circumstance. In all of the experiments, the concentration of UCNPs@PDA was fixed at 0.04 mg/mL. The stability of the UCNPs@PDA was first confirmed, as shown

Scheme 1 Principle of the biosensor based on UCNPs @ PDA and AuNPs

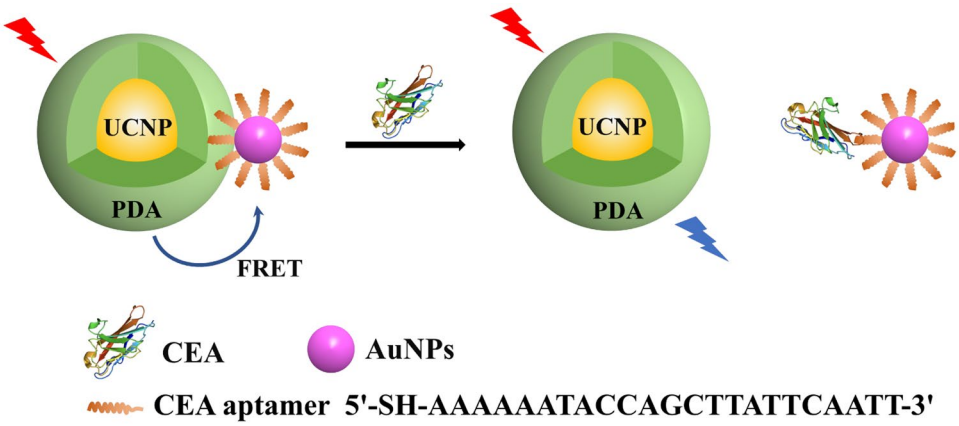

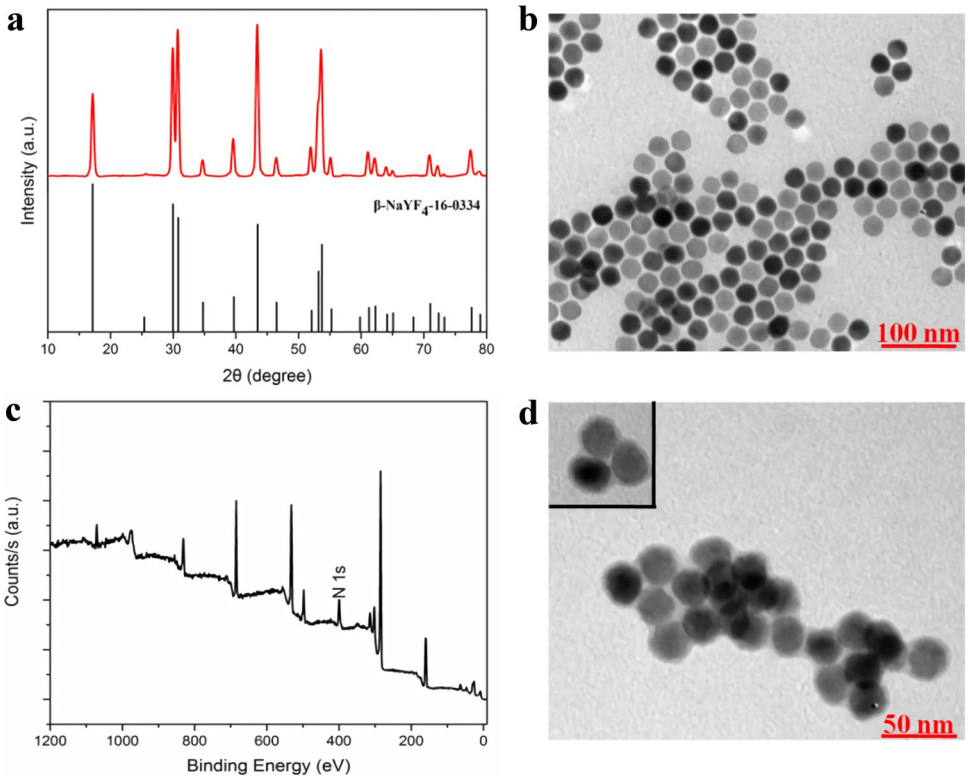

Fig. 2 **a** XRD pattern of UCNPs; **b** TEM image of UCNPs; **c** XPS spectra of UCNPs@PDA; **d** TEM image of UCNPs@PDA

in Fig. S2.† The fluorescence intensity of UCNP@PDA remained unchanged within 2 h, showing good stability and possibility to apply in subsequent detection.

It is reported that single-strand DNA has strong ability to noncovalently bind to the surface of aromatic carbon nanomaterials and assemble on its surface [30]. So that the process of energy transfer could occur between UCNPs@PDA and AuNPs-CEA aptamer through the effects of π-π stacking and hydrogen bonding between aptamer and PDA. In our experiment, as shown in Fig. S3a,† with the concentration of AuNPs-CEA aptamer increased, the fluorescence intensity of UCNPs@PDA kept decreasing (F and F_0 represent the fluorescence intensity of UCNPs@PDA at 479 nm with and without AuNPs-CEA aptamer, respectively.). Therefore, when the concentration of AuNPs-CEA aptamer concentration reached 10.4 nM, the quenching efficiency of upconversion fluorescence can reach to 90%, which was higher than those reports with organic dyes as the energy acceptors of UCNPs, where the quenching degree was about only 50% [31]. Hence, this combination of donor/acceptor pair can be a great alternative to fabricate FRET-based biosensors. The concentration of AuNPs-CEA aptamer was chosen to be 10.4 nM, in which the fluorescence quenching reached the plateau. Finally, under this condition, we examined the effect of reaction time on fluorescence quenching efficiency. As shown in Fig. S3b,† the time-dependence test showed

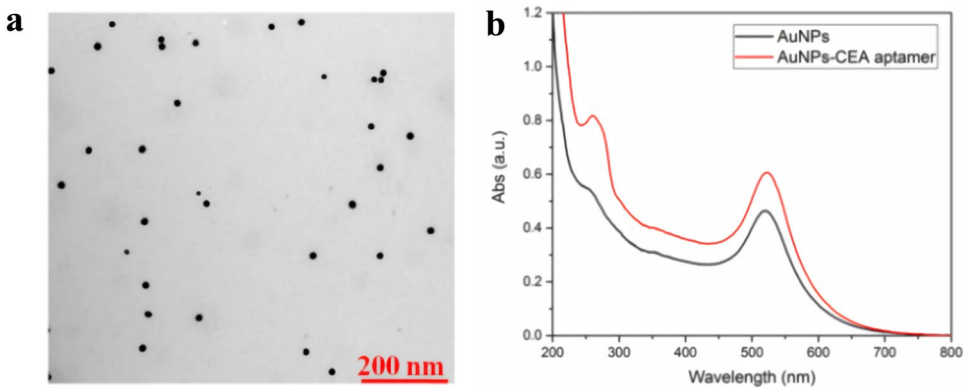

Fig. 3 **a** TEM image of AuNPs; **b** UV–vis absorption spectrum of AuNPs (black line) and AuNPs-CEA aptamer (red line)

that the biosensor needed a reaction time of 90 min to reach quenching equilibrium. Hence the reaction time of fluorescence quenching in later experiments was fixed at 90 min to ensure complete quenching and acquire stable signal.

The Detection of CEA in Aqueous Solution

After optimizing experimental conditions, we examined the performance of this biosensor for the determination of CEA in an aqueous solution. With the addition of free CEA to the system composed of UCNP@PDA and AuNPs-CEA aptamer, the aptamer was induced to combine with CEA, which weakened the π-π interaction between PDA and aptamer. Therefore, the disrupted energy transfer triggered the recovery of upconversion fluorescence. The reaction time of fluorescence recovery was investigated as shown in Fig. S4,† which indicated that the upconversion fluorescence could recover in 90 min to the maximal extent and then kept quite stable. With a fixed amount of the biosensor (0.04 mg/mL UCNPs@PDA plus 10.4 nM AuNPs-CEA aptamer), the fluorescence of UCNPs@PDA recovered with increasing amounts of CEA (Fig. 4a). More importantly, the fluorescence recovery of UCNPs@PDA was dependent on the concentration of CEA, providing opportunity to the quantitative analysis of CEA. As shown in Fig. 4b, the relative fluorescence intensity ($(F-F_0)/F_0$, where F and F_0 represents the fluorescence intensity in the presence and the absence of CEA, respectively) was linearly correlated to the logarithm of CEA concentrations in the range of 0.1–100 ng/mL. Notably, the limit of detection (LOD) was 0.031 ng / mL based on $3S_b$ / k criterion (k is the linear slope in the detection range, S_b is the standard deviation of seven blank samples), which was lower than that of most previous fluorescence probes for CEA. Compared with other fluorescent biosensors based on aptamer, our modification-free method presented a relatively lower LOD and a wider linear range for CEA (Table S1†). These experimental results indicated that it was promising to apply this biosensor in real samples.

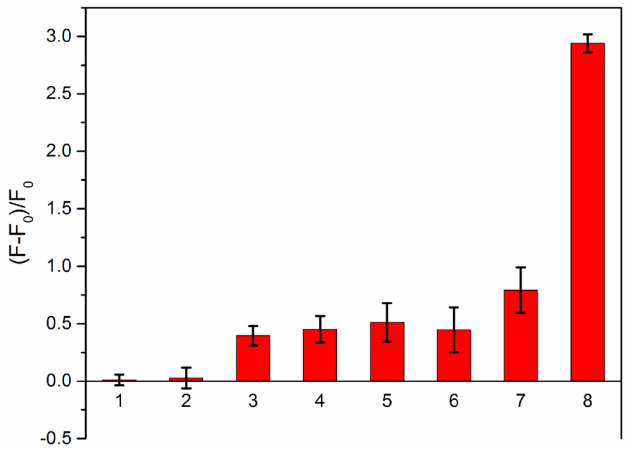

Fig. 5 Specificity studies of the biosensor toward other substances that may co-exist in serum samples (1: Ca^{2+}; 2: Na^{+}; 3: L-Cys; 4: glucose; 5: BSA; 6: albumin; 7: AFP; 8: CEA). The concentration of the species was 100 ng/mL

Specificity Assessment of the Biosensor

In order to verify the selectivity of this biosensor for CEA, we investigated the possible interference of ions, molecules

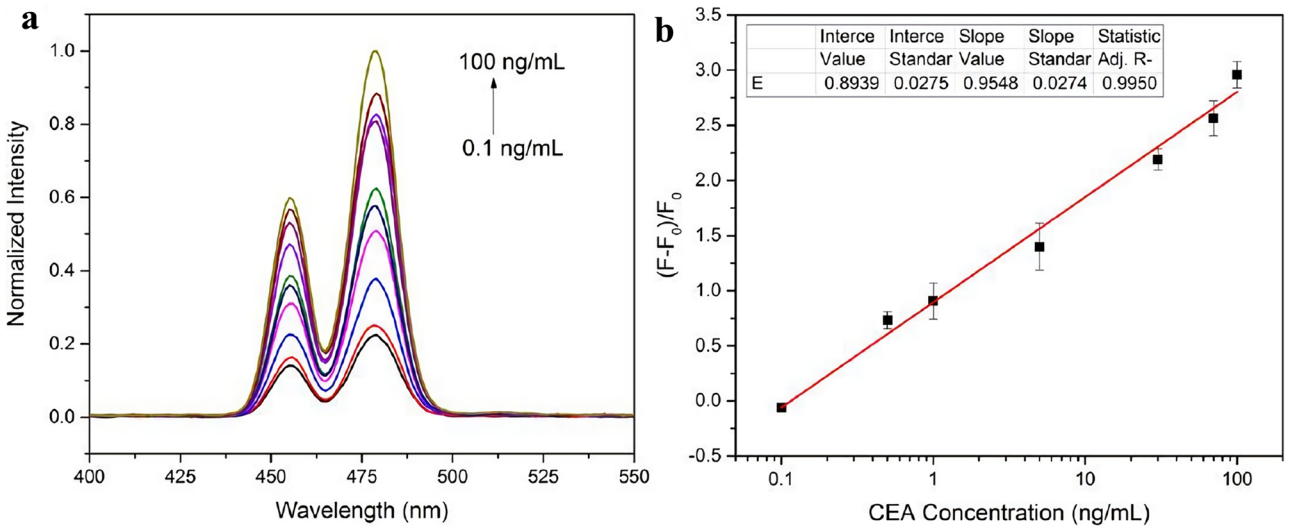

Fig. 4 **a** Fluorescence spectrum of the biosensor in aqueous solution. 0.04 mg/mL UCNPs@PDA and 10.4 nM AuNPs-CEA aptamer were used, and the concentrations of CEA tested were 0, 0.1, 0.5, 1, 5, 8, 10, 30, 70, 100 ng / mL; **b** Linear relationship between the logarithm of CEA concentrations and the fluorescence enhancement

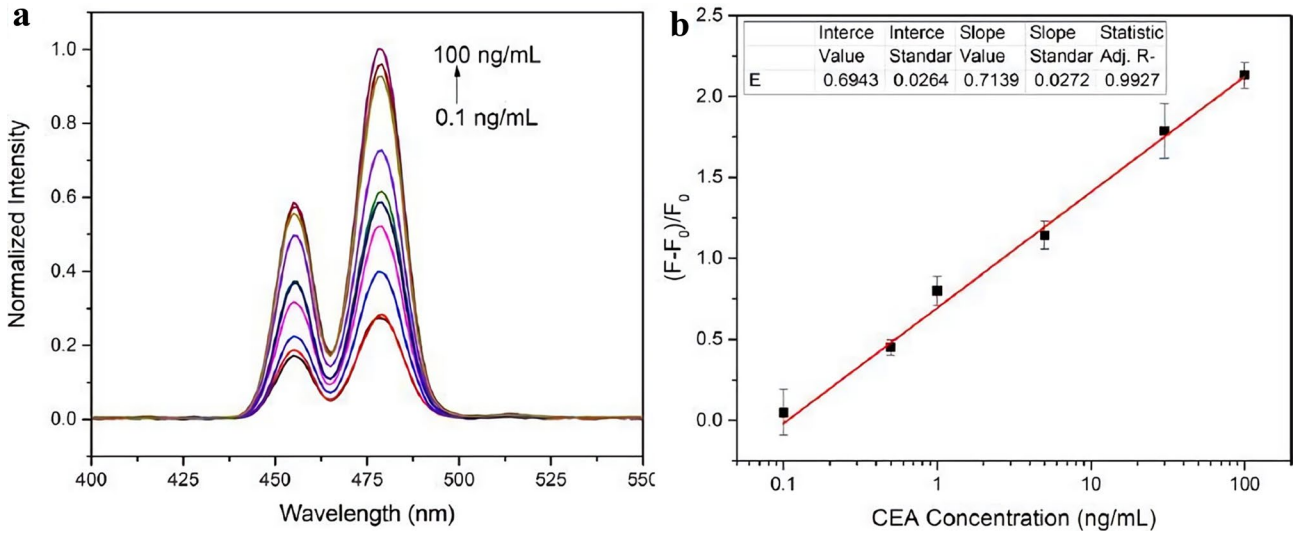

Fig. 6 **a** Fluorescence spectra of the biosensor in human serum. 0.04 mg/mL UCNPs@PDA and 10.4 nM AuNPs-CEA aptamer were used, and the concentrations of CEA tested were 0, 0.1, 0.5, 1, 5, 8, 10, 30, 70, 100 ng / mL; **b** Linear relationship between the logarithm of CEA concentrations and the fluorescence enhancement

and proteins in serum, including Ca^{2+}, Na^{+}, L-Cys, glucose, BSA, albumin, and AFP. The concentrations of these substances and CEA were both fixed at 100 ng/mL. As shown in Fig. 5, only after the addition of CEA, the fluorescence of this biosensor recovered obviously, indicating that the biosensor had good selectivity for CEA and had great possibility for CEA detection in real clinical samples like human serum.

The Detection of CEA in Human Serum

To investigate the practical applicability for monitoring CEA levels, we used the biosensor in the analysis of human serum. Generally, the concentration of CEA in healthy human beings is below 5 ng/mL [32]. With 100-fold diluted (with Tris–HCl, 10 mM, pH 7.4) human serum as the medium of assay, the influence of the original CEA in serum was negligible. Except for the changed buffer, other conditions were consistent with the experimental conditions in aqueous solution. We found that the fluorescence recovery was still correlated with the logarithm of CEA concentrations (Fig. 6b). The linear range for CEA was the same as in aqueous buffer, which was from 0.1 ng/mL to 100 ng/mL, and the LOD was 0.055 ng/mL ($3S_b/k$ criterion). These results were similar to that in aqueous solution, suggesting that the biosensor could be applicable in such complicated matrix.

Finally, standard addition experiments were conducted to verify the feasibility of this biosensor in the serum of tumour patients. Five serum samples of tumour patients were determined by the hospital, and the concentrations of CEA were reported as 48.0, 93.2, 230.4, 462.4 and 856.0 ng/mL, respectively. Before introducing these serum samples into our biosensor, they were 100-fold diluted with Tris–HCl buffer (10 mM, pH 7.4). As shown in Table S2,† the recoveries ranged from 92.6% to 107.0% with a low relative standard deviation (RSD) between 1.0 and 3.0, which are acceptable in biological samples. Above all, this biosensor has already shown potential in practical application.

Conclusions

In conclusion, we have developed a modification-free fluorescent biosensor based on UCNPs@PDA, and demonstrated its application in detecting CEA in aqueous solution and human serum. Through the coating of UCNPs with PDA, the direct binding between the phosphate gruop of DNA backbone and lanthanide ions could be inhibited, protecting the ability of aptamer to recognize the target. The PDA coated UCNPs allowed the CEA aptamer-modified AuNPs to be adsorbed onto the surface of UCNPs@PDA via the interactions of π–π stacking and hydrogen bonding, which triggered the energy transfer from UCNPs@PDA to AuNPs-CEA aptamer. In the presence of CEA, the AuNPs-CEA aptamer departed from UCNPs@PDA due to the stronger affinity of CEA with its aptamer. Thus, the recovery of upconversion fluorescence can quantify the concentration of CEA. This biosensor displays high sensitivity for CEA detection not only in aqueous solution but also in human serum, suggesting it a powerful tool for practical applications.

Supplementary Information The online version contains supplementary material available at https://doi.org/10.1007/s10895-022-02973-8.

Authors' contributions All authors contributed to the study conception and design.Material preparation, data collection and analysis were performed by Yu,Tang and Qiu. The first draft of the manuscript was edited by Zha and Liu. All authors commented on previous versions of the manuscript. All authors read and approved the final manuscript.

Funding This work was supported by [National Natural Science Foundation of China] [21906124] and Graduate Innovative Fund of Wuhan Institute of Technology.

Data Availability The authors declare that all data supporting the findings of this study are available within the article and its supplementary information files.

Declarations

Ethics Statement Not applicable.

Consent to Participate Not applicable.

Consent for Publication Not applicable.

Conflicts of interest The authors declare they have no competing interests.

References

1. Zheng W, Huang P, Tu DT, Ma E, Zhu HM, Chen XY (2015) Lanthanide-doped upconversion nano-bioprobes: electronic structures, optical properties, and biodetection. Chem Soc Rev 44:1379–1415
2. Auzel F (2004) Upconversion and anti-Stokes processes with f and d ions in solids. Chem Rev 104:139–173
3. Su QQ, Feng W, Yang DP, Li FY (2017) Resonance energy transfer in upconversion nanoplatforms for selective biodetection. Acc Chem Res 50:32–40
4. Zhang YQ, Xu S, Li XP, Zhang JS, Sun J, Tong LL, Zhong H, Xia HP, Hua RN, Chen BJ (2018) Improved LRET-based detection characters of Cu^{2+} using sandwich structured NaYF4@$NaYF_4$:Er^{3+}/Yb^{3+}@$NaYF_4$ nanoparticles as energy donor. Sensors and Actuators B-Chemical 257:829–838
5. Doughan S, Uddayasankar U, Krull UJ (2015) A paper-based resonance energy transfer nucleic acid hybridization assay using upconversion nanoparticles as donors and quantum dots as acceptors. Anal Chim Acta 878:1–8
6. Wu ZJ, Li H, Liu ZH (2015) An aptasensor for carcinoembryonic antigen based on upconversion fluorescence resonance energy transfer. Sensors and Actuators B-Chemical 206:531–537
7. Ellington AD, Szostak JW (1990) In vitro selection of RNA molecules that bind specific ligands. Nature 346:818–822
8. Tuerk C, Gold L (1990) Systematic evolution of ligands by exponential enrichment: RNA ligands to bacteriophage T4 DNA polymerase. Science (New York, N.Y.) 249:505–510
9. Stoltenburg R, Reinemann C, Strehlitz B (2007) SELEX–a (r) evolutionary method to generate high-affinity nucleic acid ligands. Biomol Eng 24:381–403
10. Fang XH, Tan WH (2010) Aptamers generated from Cell-SELEX for molecular medicine: A chemical biology approach. Acc Chem Res 43:48–57
11. Mairal T, Ozalp VC, Sanchez PL, Mir M, Katakis I, O'Sullivan CK (2008) Aptamers: molecular tools for analytical applications. Anal Bioanal Chem 390:989–1007
12. Keefe AD, Pai S, Ellington A (2010) Aptamers as therapeutics (vol 9, pg 537, 2010). Nat Rev Drug Discovery 9:8
13. Wang RW, Zhu GZ, Mei L, Xie Y, Ma HB, Ye M, Qing FL, Tan WH (2014) Automated modular synthesis of aptamer-drug conjugates for targeted drug delivery. J Am Chem Soc 136:2731–2734
14. Hicke BJ, Stephens AW, Gould T, Chang Y-F, Lynott CK, Heil J, Borkowski S, Hilger C-S, Cook G, Warren S, Schmidt PG (2006) Tumor targeting by an aptamer. Journal of nuclear medicine : official publication, Society of Nuclear Medicine 47:668–678
15. Li S, Xu LG, Sun MZ, Wu XL, Liu LQ, Kuang H, Xu CL (2017) Hybrid nanoparticle pyramids for intracellular dual microRNAs biosensing and bioimaging. Adv Mater 29:19
16. Yu Z, Ge Y, Sun Q, Pan W, Wan X, Li N, Tang B (2018) A preprotective strategy for precise tumor targeting and efficient photodynamic therapy with a switchable DNA/upconversion nanocomposite. Chem Sci 9:3563–3569
17. Chen GY, Qju HL, Prasad PN, Chen XY (2014) Upconversion nanoparticles: design, nanochemistry, and applications in theranostics. Chem Rev 114:5161–5214
18. Perlin L, MacNeil S, Rimmer S (2008) Production and performance of biomaterials containing RGD peptides. Soft Matter 4:2331–2349
19. Han S, Samanta A, Xie XJ, Huang L, Peng JJ, Park SJ, Teh DBL, Choi Y, Chang YT, All AH, Yang YM, Xing BG, Liu XG (2017) Gold and hairpin DNA functionalization of upconversion nanocrystals for imaging and in vivo drug delivery. Adv Mater 29:18
20. Qiang WB, Li W, Li XQ, Chen X, Xu DK (2014) Bioinspired polydopamine nanospheres: a superquencher for fluorescence sensing of biomolecules. Chem Sci 5:3018–3024
21. Liu XS, Cao JM, Li H, Li JY, Jin Q, Ren KF, Ji J (2013) Mussel-inspired polydopamine: a biocompatible and ultrastable coating for nanoparticles in vivo. ACS Nano 7:9384–9395
22. Ma SS, Qi YX, Jiang XQ, Chen JQ, Zhou QY, Shi GY, Zhang M (2016) Selective and sensitive monitoring of cerebral antioxidants based on the dye-labeled DNA/polydopamine conjugates. Anal Chem 88:11647–11653
23. Hammarstrom S, Engvall E, Johansson BG, Svensson S, Sundblad G, Goldstein IJ (1975) Nature of the tumor-associated determinant(s) of carcinoembryonic antigen. Proc Natl Acad Sci USA 72:1528–1532
24. Saha K, Agasti SS, Kim C, Li XN, Rotello VM (2012) Gold nanoparticles in chemical and biological sensing. Chem Rev 112:2739–2779
25. Zhang KY, Yang L, Lu F, Wu XC, Zhu JJ (2018) A universal upconversion sensing platform for the sensitive detection of tumour-related ncRNA through an exo III-assisted cycling amplification strategy. Small 14:10
26. Wang F, Deng RR, Liu XG (2014) Preparation of core-shell NaGdF4 nanoparticles doped with luminescent lanthanide ions to be used as upconversion-based probes. Nat Protoc 9:1634–1644
27. Liu FY, He XX, Lei Z, Liu L, Zhang JP, You HP, Zhang HM, Wang ZX (2015) Facile preparation of doxorubicin-loaded upconversion@polydopamine nanoplatforms for simultaneous in vivo multimodality imaging and chemophotothermal synergistic therapy. Adv Healthcare Mater 4:559–568
28. Haiss W, Thanh NTK, Aveyard J, Fernig DG (2007) Determination of size and concentration of gold nanoparticles from UV-vis spectra. Anal Chem 79:4215–4221

29. Liu J, Lu Y (2006) Preparation of aptamer-linked gold nanoparticle purple aggregates for colorimetric sensing of analytes. Nat Protoc 1:246–252
30. Zheng M, Jagota A, Semke ED, Diner BA, McLean RS, Lustig SR, Richardson RE, Tassi NG (2003) DNA-assisted dispersion and separation of carbon nanotubes. Nat Mater 2:338–342
31. Wang CL, Li XM, Zhang F (2016) Bioapplications and biotechnologies of upconversion nanoparticle-based nanosensors. Analyst 141:3601–3620
32. Wang DF, Li YY, Lin ZY, Qiu B, Guo LH (2015) Surface-enhanced electrochemiluminescence of $Ru@SiO_2$ for ultrasensitive detection of carcinoembryonic antigen. Anal Chem 87:5966–5972